ResearchGate

See discussions, stats, and author profiles for this publication at:
https://www.researchgate.net/publication/244327179

Photodissociation of CFCl3 at 193 nm investigated by photofragment translational spectroscopy

ARTICLE *in* CHEMICAL PHYSICS LETTERS · JANUARY 1996

Impact Factor: 1.9 · DOI: 10.1016/0301-0104(95)00271-5

CITATIONS
24

READS
5

2 AUTHORS:

Jeremy Graham Frey
University of Southampton
183 PUBLICATIONS **1,496** CITATIONS
SEE PROFILE

Peter Felder
University of Zurich
51 PUBLICATIONS **1,257** CITATIONS
SEE PROFILE

Available from: Peter Felder
Retrieved on: 25 January 2016

ELSEVIER

Chemical Physics 202 (1996) 397–406

Chemical Physics

Photodissociation of CS_2 at 193 nm investigated by polarised photofragment translational spectroscopy

Jeremy G. Frey [b], Peter Felder [a,*]

[a] *Physikalisch-Chemisches Institut der Universität Zürich, Winterthurerstrasse 190, CH-8057 Zürich, Switzerland*
[b] *Department of Chemistry, University of Southampton, Southampton SO17 1BJ, UK*

Received 8 June 1995

Abstract

The predissociation dynamics of CS_2 in the $\tilde{A}(^1B_2)$ state have been investigated by means of high resolution photofragment translational spectroscopy at 193 nm. The photofragment translational energy distributions derived from the time-of-flight (TOF) distributions of the CS fragment are qualitatively similar to the ones obtained in previous investigations. Detailed measurements carried out with a linearly polarised photolysis laser reveal a pronounced anisotropy of the fragment recoil which is dependent on the translational energy and on the molecular beam carrier gas. It is possible to partition each TOF distribution of the CS fragment into two components corresponding to the formation of $S(^3P)$ and $S(^1D)$ partner fragments, respectively, in a manner consistent with recent branching ratio determinations. In the case of the Ne beam this partitioning leads to the anisotropy parameters $\beta(S\ ^1D) \approx 0.2$ and $\beta(S\ ^3P) \approx 1.0$. These results indicate that the overall photodissociation process occurs on a time scale of ~ 1.5 ps and that the formation of $CS + S(^1D)$ proceeds through a strongly bent transition state.

1. Introduction

Small molecules with diffuse vibrational structure in the ultraviolet absorption spectrum have recently received considerable attention with regard to their predissociation dynamics [1–5] and the possibility of mode-specific photodissociation [6–11]. In this respect, the photodissociation of carbon disulfide (CS_2) in the wavelength region between 185 and 225 nm is particularly interesting. The pertinent $S_3 \leftarrow S_0$ electronic transition leads from the linear ground state $\tilde{X}(^1\Sigma_g^+)$ to the bent upper state $\tilde{A}(^1B_2)$, which is correlated with the $^1\Sigma_u^+$ state of the linear configuration [12,13]. The change from linear to bent geometry, combined with a rather deep potential well in the $\tilde{A}$ state, leads to a rich vibrational structure in the absorption spectrum. The diffuseness of these spectral features and the rapid drop of the fluorescence quantum yield at excitation wavelengths shorter than 215 nm [14] have been attributed to an efficient predissociation process [12,13]. This can proceed either via the energetically most favourable but spin-forbidden reaction

$$CS_2 \xrightarrow{h\nu} CS(X\ ^1\Sigma^+) + S(^3P_J) \qquad (1)$$

* Corresponding author.

0301-0104/96/$15.00 © 1996 Elsevier Science B.V. All rights reserved
SSDI 0301-0104(95)00271-5

or via the spin-allowed but more endothermic reaction

$$CS_2 \xrightarrow{h\nu} CS(X\,^1\Sigma^+) + S(^1D_2). \quad (2)$$

No other dissociation channels are accessible at the photon energies of the $\tilde{A} \leftarrow \tilde{X}$ transition.

The time scale τ of CS_2 predissociation has recently been studied by Baronavski and Owrutsky [15]. Using a femtosecond pump and probe technique these authors measured the lifetime of the $\tilde{A}$ state photoexcited at 205 nm to be 600 ± 100 fs. This result indicates that previous determinations of τ with indirect methods such as the measurement of absorption linewidths by laser induced fluorescence (LIF) [16] or the analysis of photo-fragment angular distributions [17,18] have provided lifetime estimates that are generally too long. In contrast, resonance Raman depolarisation ratios [19] yield lifetimes that are in excellent agreement with the femtosecond experiment [15] and furthermore show a sharp decrease of τ with increasing photon energy. In view of this energy dependence, the lifetime of CS_2 excited at wavelengths near 193 nm is expected to be less than 500 fs.

Several groups have investigated the photodissociation of CS_2 at 193 nm using an ArF excimer laser as the photolysis source [16–18,20–24]. Until 1988, there has been no satisfactory agreement between these studies, most notably concerning the relative yield of the $S(^3P)$ and $S(^1D)$ atoms and the vibrational distributions of their CS partner fragments. However, the combined results of a high resolution photofragment translational spectroscopy (PTS) investigation by Tzeng et al. [22] and a LIF Doppler study of nascent S atoms by Waller and Hepburn [18] have led to a more consistent picture. According to the LIF results the branching ratio between the two dissociation pathways (1) and (2) is $S(^3P)/S(^1D) = 2.8 \pm 0.3$ [18], which is substantially larger than the values obtained in earlier investigations [17,20,21,23]. Using the branching ratio determined by Waller and Hepburn, the photofragment translational energy distribution measured in the PTS experiment of Tzeng et al. was split up into the contributions from reactions (1) and (2) and the corresponding vibrational distributions of the CS fragments were then estimated by applying an energy balance [22]. As a main new result, the CS fragments produced in coincidence with ground state sulfur atoms $S(^3P)$ were concluded to contain up to 13 vibrational quanta.

More recently, the $S(^3P)/S(^1D)$ ratio has also been studied at slightly longer wavelengths [11]. By carefully measuring the LIF signals of $S(^3P_J, J = 2, 1, 0)$ and $S(^1D_2)$ as a function of photolysis wavelength in the spectral range between 198 and 215 nm, Starrs et al. [11] were able to show that the $S(^3P)/S(^1D)$ ratio as well as the populations of the $S(^3P_J)$ sublevels are sensitively dependent on the type of ro-vibronic band excited in the parent. These observations indicate the presence of several interacting excited electronic states.

In contrast to the isotropic fragment distribution obtained in an early PTS study at 193 nm by Yang et al. [17], the Doppler profiles measured at the same photolysis wavelength by Waller and Hepburn [18] show clear evidence of an anisotropic recoil distribution. The apparent discrepancy between the two experiments was rationalized by the fact that the LIF measurements [18] were carried out with jet-cooled CS_2, whereas a room temperature effusive beam was used in the PTS study [17]. With an excited state lifetime of 2 ps, the rotational motion of the parent molecules would indeed be expected to cause a nearly isotropic angular distribution of the fragments produced in the effusive beam at 300 K, but not in the supersonic jet with $T \approx 20$ K [18]. However, since the direct lifetime measurements by Baronavski and Owrutsky [15] indicate that the excited state lifetime at 193 nm is substantially shorter than 2 ps, the questions concerning the above mentioned anisotropy measurements re-emerge. As a matter of fact, the classical interpretation of the anisotropy parameter β may well be inappropriate at the low rotational temperatures attained in a supersonic beam, particularly if interacting electronic states are involved [25–27].

In order to obtain further information on the photofragment anisotropy of CS_2 we have undertaken a high resolution PTS study with a linearly polarised photolysis laser. While not providing a state selective detection of the sulfur atom such as in the LIF experiments by Waller and Hepburn [18], our measurements allow us to determine the

anisotropy parameter with higher accuracy and as a function of the photofragment translational energy.

2. Experimental

The experiments were carried out with a high-resolution PTS apparatus [28,29] featuring a rotatable pulsed molecular beam source and a spatially fixed detector. A pulsed supersonic beam of CS_2 was intersected by the linearly polarised radiation of an ArF excimer laser (Lambda Physik EMG 101 MSC) and the resulting photofragments were detected after travelling through a flight path of 34.5 cm. The molecular beam was generated by means of a piezoelectrically driven valve with an orifice diameter of 0.3 mm. Premixed gas samples of 5% CS_2 seeded either in helium or neon carrier gas at a total stagnation pressure of 400 mbar were used throughout this study and the molecular beam velocity distribution was measured by laser induced hole burning [30]. The parameters of the distribution $f(v) = C \exp[-(v - v_0)^2/\alpha^2]$ were determined to be $\alpha = 91$ m/s and $v_0 = 1230$ m/s for CS_2 seeded in He, whereas $\alpha = 44$ m/s and $v_0 = 760$ m/s for CS_2 seeded in Ne. The corresponding speed ratios $S = v_0/\alpha$ are 13.5 and 17.5, respectively.

The photolysis laser was directed through a stacked-plates polariser followed by a zeroth-order half-wave retarder (B. Halle, Berlin) mounted on a rotation stage. The laser beam was collimated and mildly focused to a spot size of 2.5×2.5 mm^2 at the intersection with the molecular beam and the pulse energy was maintained at 5 mJ. The laser polarisation degree, defined here as the intensity of the desired polarisation divided by the total laser intensity, was measured with a Brewster plate inserted at the beam crossing point and was found to be $92 \pm 1\%$.

The photofragment TOF distributions were generally obtained at a given angle Θ of the molecular beam source and various laser polarisation angles ϵ, with both angles being defined with respect to the laboratory-fixed direction of the detector axis. The photolysis products CS and S are detected with the mass filter set at $m/e = 44$ (CS^+) and $m/e = 32$ (S^+), respectively. However, since the TOF signal at $m/e = 32$ is complicated by the contribution from CS radicals that are cracked to S^+ in the electron bombardment ioniser, the final TOF data were collected exclusively at $m/e = 44$. A time offset of 26 μs due to the ion flight time of CS^+ through the mass filter has been subtracted in all the TOF distributions shown in the next section.

3. Data analysis

The recoil distribution of the fragment pairs formed upon the photolysis of an ensemble of randomly oriented parent molecules is expressed with the general form

$$f(E_T, \theta) = P(E_T) w(\theta, E_T), \tag{3}$$

in which $P(E_T)$ is the total translational energy, θ is the angle between the recoil direction and the laser polarisation, and

$$w(\theta, E_T) = \frac{1}{4\pi}[1 + \beta(E_T) P_2(\cos\theta)] \tag{4}$$

is the angular distribution appropriate for a one-photon process [31]. The anisotropy parameter β is constrained to the range between -1 and $+2$, and its dependence on E_T, while often difficult to measure, accounts for the fact that the energy and angular variables are not necessarily separable.

The recoil distribution (3) was determined by means of a least squares forward convolution procedure that is described in detail elsewhere [32]. The functions $P(E_T)$ and $\beta(E_T)$ were approximated by a suitably chosen set of cubic splines and polynomials, respectively, whose coefficients were optimised with an automatic fitting algorithm [32]. This involves the calculation of TOF distributions and subsequent refinement of $P(E_T)$ and $\beta(E_T)$ until the best agreement between calculated and experimental TOF data is attained. The transformation from the CM to the LAB frame and the averaging effects caused by the spread in molecular beam velocities and by the finite experimental resolution are appropriately taken into account [33]. The advantage of this approach is that it allows one to determine the best fit of a set of polarised and unpolarised TOF distributions. Moreover, it is possible to obtain statistical error bounds for the $P(E_T)$ and $\beta(E_T)$ distributions.

The fitting procedure is particularly simple if the angular distribution is isotropic or if β is independent of E_T [32]. Accordingly, most of the polarised TOF data were recorded as pairs with mutually orthogonal polarisations, thus allowing to construct the unpolarised distributions by summation of the polarised signals. The unpolarised distributions and the sums of the orthogonal pairs of polarised TOF distributions were used to obtain an "unpolarised" $P(E_T)$ which was then used together with the difference between the members of a polarised TOF pair to generate a fit to $\beta(E_T)$ and thus obtain the isotropic $P(E_T)$.

4. Results

The polarised TOF spectra of the CS fragment recorded with the LAB angle $\Theta = 21°$ and various laser polarisation angles ϵ are displayed in Fig. 1. In the case of CS_2 seeded in He (see Fig. 1a) the photofragment signal is maximal at $\epsilon = 150°$ and minimal at $\epsilon = 60°$. Taking into account the transformation from the CM to the LAB system [34], the observed angular dependence implies a *positive anisotropy parameter* β. This is confirmed by the measurements with CS_2 seeded in Ne, where the photofragment signal at $\epsilon = 70°$ is substantially stronger than the one at 160° (see Fig. 1b). The dependence of β on the translational energy will be addressed further below. The *unpolarised* TOF distributions obtained by summation of the polarised spectra of Figs. 1a and 1b, are shown in Figs. 2a and 2b, respectively. As already observed by Tzeng et al. in their PTS study with an unpolarised ArF laser [22], the TOF signals show a rich structure which reflects the formation of singlet and triplet S atoms in coincidence with CS fragments in various vibrational states.

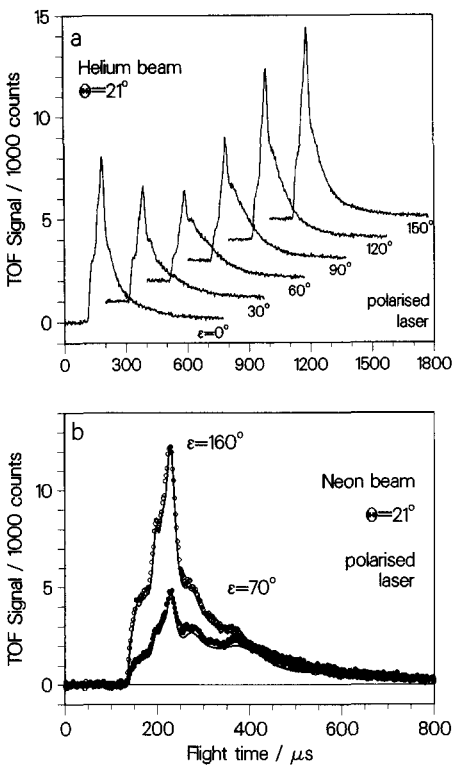

Fig. 1. Polarised TOF distributions of the CS fragment ($m/e = 44$) measured with the LAB angle $\Theta = 21°$ and different laser polarisation angles ϵ. (a) CS_2 seeded in He. (b) CS_2 seeded in Ne. The solid lines are the calculated TOF distributions obtained from the best-fitting recoil distributions given in Fig. 4.

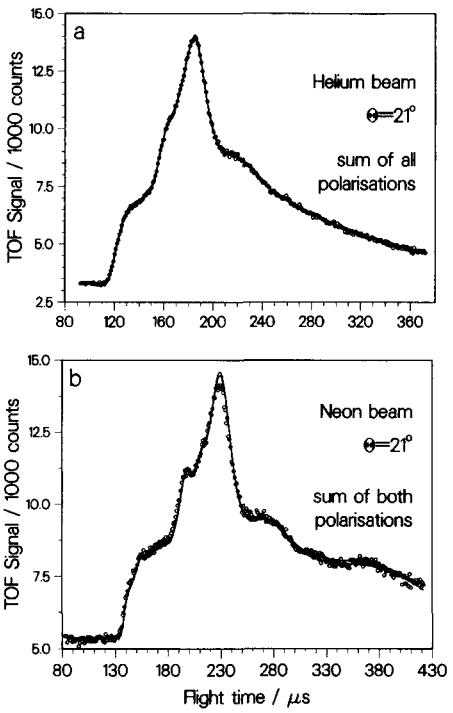

Fig. 2. Unpolarised TOF distributions of the CS fragment ($m/e = 44$) obtained by summation of the polarised TOF signals given in Fig. 1. (a) CS_2 seeded in He. (b) CS_2 seeded in Ne. The solid lines are the calculated TOF distributions obtained from the best-fitting recoil distributions given in Figs. 4 and 5.

The forward convolution analysis described in Section 3 was applied separately to the TOF data sets obtained with He and Ne carrier gas in order to determine the respective best-fitting recoil distributions. In the case of the He beam, the analysis was carried out with the six polarised TOF distributions measured with $\Theta = 21°$ (see Fig. 1a), whereas in the case of the Ne beam, the two polarized TOF spectra recorded with $\Theta = 21°$ (see Fig. 1b) were analysed in conjunction with the unpolarised TOF spectrum obtained with $\Theta = 51°$, which is displayed in Fig. 3a. The best-fitting recoil distributions $\beta(E_T)$ and $P(E_T)$ are shown in Figs. 4 (neon) and 5 (helium) along with the statistical error bounds corresponding to ± 2 standard deviations. Because of the lower molecular beam velocity and the inclusion of the large angle scattering measurement with $\Theta = 51°$, the distributions obtained from the neon data have

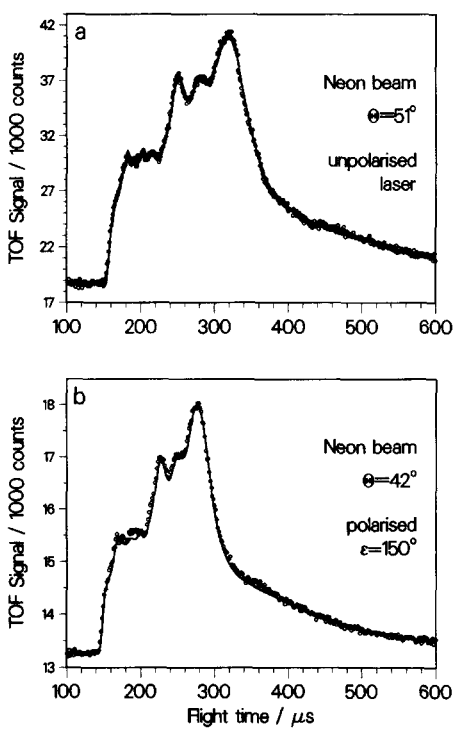

Fig. 3. TOF distributions of the CS fragment ($m/e = 44$) measured at larger scattering angles. (a) CS_2 seeded in Ne, $\Theta = 51°$, unpolarised laser. (b) CS_2 seeded in Ne, $\Theta = 42°$, polarised laser with $\epsilon = 150°$, favouring parallel recoil. The solid lines are the calculated TOF distributions obtained from the best-fitting recoil distributions given in Fig. 4.

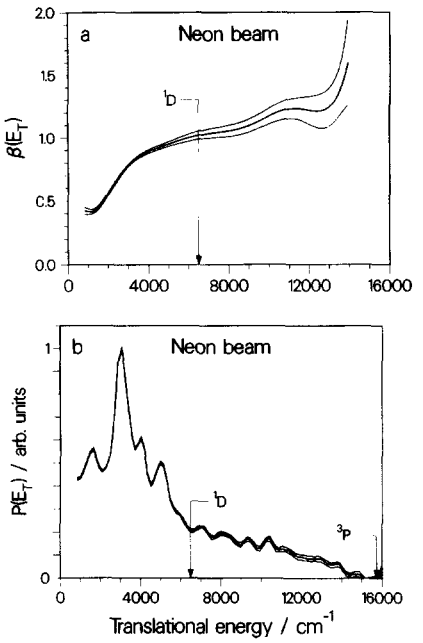

Fig. 4. Photodissociation of CS_2 at 193 nm. Recoil distributions derived from a global fit to the TOF data obtained with Ne carrier gas. (a) Anisotropy parameter β versus total translational energy. (b) Total translational energy distribution $P(E_T)$ of the fragment pairs CS + S. The vertical arrows indicate the energy thresholds for the formation of $CS(v = 0, J = 0)$ with $S(^3P_2)$ and $S(^1D_2)$, respectively. Error bounds represent $\pm 2\%$ standard deviations.

narrower error bounds and a better kinetic energy resolution than those derived from the helium data. In particular, the translational energy distribution $P(E_T)$ pertaining to the neon data (Fig. 4b) exhibits a multitude of well defined vibrational features; these are better resolved than in the previous high resolution study by Tzeng et al. [22] and, moreover, we see clear evidence for a peak at low translational energy $E_T \approx 600$ cm^{-1}. The $P(E_T)$ obtained with helium (Fig. 5b) has significantly wider error bounds than, but is otherwise consistent with, the neon data. The anisotropy distribution $\beta(E_T)$ shows for both carrier gases a decreasing trend from higher to lower translational energy with a superimposed undulatory behaviour (see Figs. 4a and 5a). Clearly, however, the neon data show a more pronounced anisotropy than the helium data.

The adequacy of the best-fitting recoil distributions is demonstrated with the TOF distributions calculated therefrom. These are displayed as solid

lines in Figs. 1, 2, and 3a and are seen to be in good agreement with the experimental distributions. A further TOF spectrum measured with CS_2 seeded in Ne using $\Theta = 42°$ and a single polarisation angle $\epsilon = 150°$ is displayed in Fig. 3b. Although not included in the data set used for the fitting procedure, this spectrum is well reproduced by the simulation and hence provides a consistency test of the recoil distributions given in Fig. 5.

Finally, we address the possibility of an angular offset in the distribution (4). Such an offset might arise as a consequence of interference effects in multisurface photodissociation [26,35]. Therefore, we applied an alternative analysis method [36] to the polarised TOF data given in Fig. 1a. For every flight time channel t, the signal $N(\epsilon; t)$ as a function of ϵ was fitted to the analytical form

$$N(\epsilon; t) = N_{iso}(t)\{1 + \beta(t)P_2[\cos(\theta(\epsilon; t) - \theta_0(t))]\}, \quad (5)$$

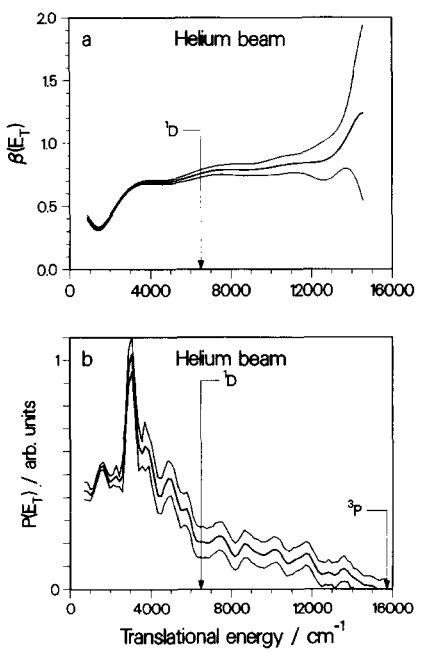

Fig. 5. Photodissociation of CS_2 at 193 nm. Recoil distributions derived from a global fit to the TOF data obtained with He carrier gas. (a) Anisotropy parameter β versus total translational energy. (b) Total translational energy distribution $P(E_T)$ of the fragment pairs CS + S. The vertical arrows indicate the energy thresholds for the formation of $CS(v = 0, J = 0)$ with $S(^3P_2)$ and $S(^1D_2)$, respectively. Error bounds represent ±2% standard deviations.

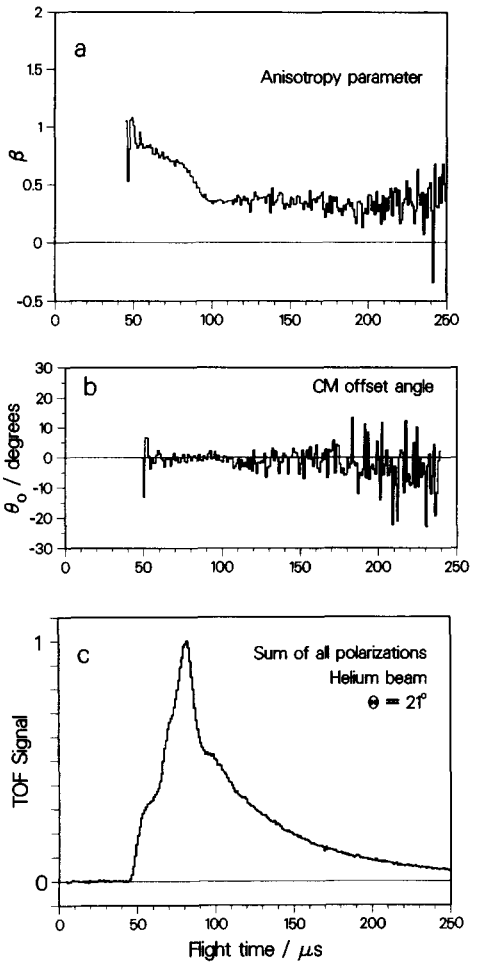

Fig. 6. Photodissociation of CS_2 seeded in He. (a) Anisotropy parameter β and (b) offset angle θ_0 derived by fitting the polarised TOF data of Fig. 1a to Eq. (5) in the text. The unpolarised TOF signal (c) is shown for comparison.

where the fitting parameters $N_{iso}(t)$, $\beta(t)$ and $\theta_0(t)$ represent the isotropic TOF signal, anisotropy parameter and angular offset angle, respectively. It is noted that for a given polarisation angle ϵ in the LAB system, the corresponding angle θ in the CM frame depends on the photofragment velocity and hence on the flight time t. After correction for the kinematic averaging effects and the incomplete laser polarisation, the anisotropy distribution $\beta(t)$ displayed in Fig. 6a was obtained. Taking into account the distortion caused by the strongly nonlinear relation between flight time and translational energy, the distribution $\beta(t)$ is found to be consistent with

$\beta(E_T)$ determined in the global data analysis. The offset angle $\theta_0(t)$ is shown in Fig. 6b. Disregarding the fluctuations at long flight times, where the TOF signal is low (cf. Fig. 6c) and the LAB to CM transformation is poorly defined because of the small recoil velocity, the offset angle is found to be essentially zero.

5. Discussion

The energy balance of the photodissociation process is given by

$$h\nu + D_0 = E(S) + E(CS) + E_T, \quad (6)$$

where the small internal energy of the CS_2 molecules in the supersonic beam has been neglected. For a given electronic state of the S atom, the total translational energy is therefore related to the internal energy of the CS fragment according to

$$E_T = h\nu + D_0 - E(S) - E(CS) = E_{avl}^{(i)} - E(CS). \quad (7)$$

Inserting the dissociation energy $D_0 = 36000 \pm 100$ cm^{-1} [37], the laser photon energy $h\nu = 51730$ cm^{-1} and the appropriate electronic energy of the sulfur atom, $E(S\ ^3P_2) = 0$ and $E(S\ ^1D_2) = 9240$ cm^{-1} [38], we obtain the maximum translational energy thresholds of the two dissociation channels, $E_{avl}^{(1)} = 15730$ cm^{-1} and $E_{avl}^{(2)} = 6490$ cm^{-1}. Accordingly, any photofragments formed with a total translational energy larger than 6490 cm^{-1} are unambiguously attributed to the triplet dissociation channel (1). As shown in Figs. 4b and 5b, and already found in previous PTS investigations [17,20–22], the $P(E_T)$ distribution exhibits a steep increase just below the threshold of reaction (2), suggesting at first glance that this process is the dominant decay pathway. However, because any CS fragments formed in reaction (1) with high vibrational energy ($v > 7$) also produce a TOF signal at low translational energy, the partitioning of $P(E_T)$ into its contributions from reactions (1) and (2) can only be made by taking into account additional information from other experiments. Indeed, Waller and Hepburn [18] found by spectroscopic probing of the S atoms that reaction (1) and not reaction (2) is the main dissociation channel. Based on the branching ratio $S(^3P)/S(^1D) = 2.8 \pm 0.3$ determined by Waller and Hepburn [18], Tzeng et al. [22] concluded that the contribution of the triplet channel (1) to the photofragment signal at translational energies below $E_{avl}^{(2)}$ is by no means negligible (see Fig. 5b in Ref. [22]), in contrast to the assumption made in earlier PTS studies [17,21]. However, the exact *shape* of the two $P(E_T)$ components and hence the internal energy distributions of the CS fragments formed in reactions (1) and (2) remain uncertain.

In previous investigations [36,39,40] we have demonstrated that accurate measurements of the anisotropy as a function of recoil energy can supply the information required to disentangle the overlapping TOF signals of two competing dissociation channels, provided that these have sufficiently different β parameters and provided that for a given dissociation channel the value of β is independent of E_T. According to the polarisation dependent Doppler profiles measured by Waller and Hepburn [18], the photofragment angular distributions of the two dissociation channels are characterised by $\beta(1) = 0.85 \pm 0.15$ and $\beta(2) = 0.99 \pm 0.15$. Because of the rather large error bars, it was not obvious beforehand whether the above mentioned conditions for a signal partitioning are fulfilled in the case of CS_2.

We now consider the anisotropy distributions determined in our experiment. Starting with the translational energy region above $E_{avl}^{(2)}$, where the signal necessarily originates from the triplet channel (1), we first note that β is definitely larger with the Ne beam than with the He beam. For example, at $E_T = 8000$ cm^{-1} we observe $\beta_{Ne} = 1.05 \pm 0.05$ and $\beta_{He} = 0.78 \pm 0.03$, respectively. Second, the anisotropy measured with the Ne beam decreases from $\beta_{Ne} \approx 1.3$ at $E_T = 13500$ cm^{-1} to $\beta_{Ne} = 1.0$ at $E_T = 6500$ cm^{-1} just above the threshold of $S(^1D_2)$ formation. A similar trend is observed with the He beam, although the larger error bounds leave considerable uncertainty with regard to the slope of $\beta(E_T)$. The only plausible cause for the first finding is a difference in the rotational temperature of the parent molecules in the two beams, although the actual mechanism remains to be discussed. LIF experiments carried out in this laboratory with CS_2 seeded in Ne and beam conditions similar to ours gave a rotational temperature of 10 K [41]. With He carrier gas the

rotational cooling is not as efficient [42] and we hence expect a rotational temperature close to 20 K.

The angular distribution of photofragment recoil has traditionally been discussed in terms of simple classical mechanical models [31,34,43,44]. In the present case the anisotropy parameter can be written as

$$\beta = 2P_2(\cos\chi)\frac{P_2(\cos\alpha) + \omega^2\tau^2 - 3\omega\tau\sin\alpha\cos\alpha}{1+4\omega^2\tau^2}, \quad (8)$$

where χ is the effective angle between the electronic transition moment μ and the final recoil velocity v in the CM system, ω is the angular frequency of the parent rotation and τ is the average lifetime of the excited molecule. The angle α is defined as

$$\alpha = \arcsin\left(\frac{v_t}{v}\right), \quad (9)$$

with v_t denoting the tangential velocity of the rotating molecule.

In simple terms, the factor $2P_2(\cos\chi)$ on the right-hand side of (8) accounts for the dissociation geometry whereas the rightmost factor represents the anisotropy reduction caused by rotational reorientation of the dissociation complex and by non-axial fragment recoil. However, this latter effect turns out to be negligible over the whole range of translational energies observable in our experiment. Even if we assume the rotational temperature of CS_2 seeded in He to be as high as 20 K and consider a translational energy of merely 1000 cm^{-1}, the tangential velocity $v_t \approx 70$ m/s is substantially smaller than the recoil velocity $v = 1170$ m/s, hence implying a very small deviation from axial recoil ($\alpha \approx 3.5°$) which thus cannot account for the decreasing trend of $\beta(E_T)$ towards lower translational energy. Therefore, we propose that the kinetic energy dependence of β is due to the overlap of the two reaction channels (1) and (2). Obviously, the assumption of a constant β for each dissociation channel is not strictly fulfilled since, as noted above, β already shows some variation in the region where only the triplet channel (1) can contribute to the signal. However, in view of the rather large error bars in that region, we *assumed* that in the energy range below $E_{avl}^{(2)}$ the anisotropy parameter can be adequately expressed as

$$\beta(E_T) = x(E_T)\beta_P + [1 - x(E_T)]\beta_D, \quad (10)$$

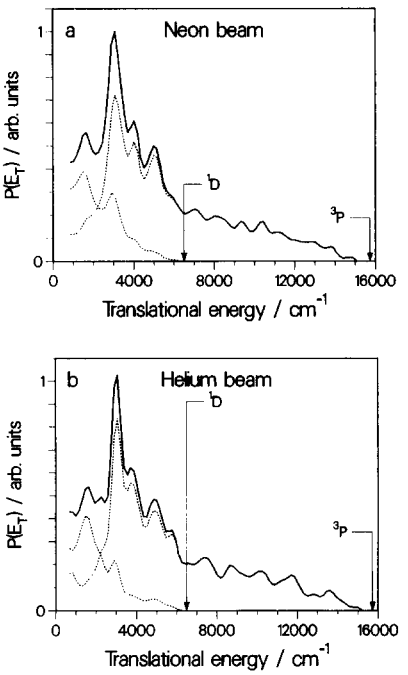

Fig. 7. Partitioning of the total translational energy distribution $P(E_T)$ into contributions of reactions (1) and (2). (a) Neon beam, $\beta_P = 1.0$, $\beta_D = 0.2$. (a) Helium beam, $\beta_P = 0.75$, $\beta_D = 0.2$.

where β_P and β_D are *constant* and pertain to the reactions forming $S(^3P)$ and $S(^1D)$, respectively. The coefficient $x(E_T)$ represents the relative contribution of the triplet channel (1) to the total photoframent signal at a given translational energy E_T. For given values of β_P and β_D the function $x(E_T)$ is readily calculated from the observed anisotropy distribution $\beta(E_T)$.

The parameters β_P and β_D were chosen as follows. The value of β_P was set equal to the anisotropy parameter measured just above $E_{avl}^{(2)}$, where the contribution of the singlet reaction (2) is necessarily zero. This gave $\beta_P(Ne) = 1.02$ and $\beta_P(He) = 0.75$. The value of β_D was then varied systematically until the partitioning between reactions (1) and (2) was consistent with the branching ratio $S(^3P)/S(^1D) = 2.8$ determined spectroscopically by Waller and Hepburn [18]. For the Ne data this was achieved with $\beta_D = 0.2$ and gave the component distributions shown in Fig. 7a. The same value of β_D was applied to the He data and gave partitioning shown in Fig. 7b, which is quite similar to that in Fig. 7a.

As the electronic transition involved in the photolysis at 193 nm leads from the linear ground state $\tilde{X}(^1\Sigma_g^+)$ to high vibrational levels above the barrier to linearity of the bent electronic state $\tilde{A}(^1B_2)$, the transition dipole moment is oriented along the symmetry axis of the linear molecule, like in a $(^1\Sigma_u^+) \leftarrow (^1\Sigma_g^+)$ transition. In the limit of prompt dissociation the anisotropy parameter should thus be equal to $+2$, as seen by inserting $\omega\tau \approx 0$ and $\chi = 0$ into Eq. (8). Since the experimentally determined parameters β_P and β_D are significantly smaller than this limiting value, we should consider the effects of a finite lifetime and non-linear geometry of the excited molecule, which both lead to a reduction of β. Based on recent experiments [15,19] the dissociation at 193 nm is expected to occur within ~ 500 fs. With rotational temperatures of 10 K in the Ne beam and of 20 K in the He beam, this leads to estimates $\omega\tau \approx 0.15$ and 0.2, respectively, from which one obtains $\beta_{Ne} \approx 1.9\ P_2(\cos\ \chi)$ and $\beta_{He} \approx 1.8\ P_2(\cos\ \chi)$. It turns out that in order to reproduce our experimental β values one would have to invoke unrealistically large distortions from linearity. However, it should be considered that both the time resolved experiment [15] and the Raman depolarisation measurement [19] actually monitor the *disappearance* of the initially excited S_3 state. If we assume that the *overall process*, involving photoexcitation, predissociation and evolution on the final potential energy surface until the photofragments cease to interact, requires a time of the order of 1.5 ps rather than 500 fs, we obtain $\beta_{Ne} \approx 1.3\ P_2(\cos\ \chi)$ and $\beta_{He} \approx 1.1\ P_2(\cos\ \chi)$. These expressions closely agree with the β_P values measured at high translational energy, if we insert $\chi \approx 0$. In other words, dissociation through the triplet channel appears to proceed mainly in the linear configuration. In contrast, the substantially reduced anisotropy β_D of the singlet channel strongly points to a bent dissociation mode. This is not unreasonable if one considers that the predissociation leading to the $S(^1D)$ product necessarily involves a different final electronic state than the one leading to $S(^3P)$ and therefore proceeds along an entirely different pathway.

If the formation of $S(^1D)$ proceeds through a strongly bent intermediate or final electronic state, it seems likely that the the pertinent non-adiabatic transition is restricted to occur at large bending angles, hence leading to a low value of β_D. Such a restricted dissociation pathway may also account for the fact that the quantum yield of the spin-allowed singlet channel is substantially smaller than that of the spin-forbidden triplet channel.

There is some evidence in our data for an energy dependent β value in the high translational energy region above 8000 cm^{-1}. The undulatory structure may reflect the complexities of the triplet channel where both the $S(^3P_2)$ and $S(^3P_1)$ states are known to be formed with substantial yield. Since the energy separation of these states (396 cm^{-1} [38]) is of a similar order of magnitude as the vibrational energy of the CS fragment, there exist various possibilities of quantum mechanical resonances and interferences [25–27,35] between the $S(^3P_2)$ and $S(^3P_1)$ dissociation channels.

Further insight might be gained from experiments with a higher resolution tunable photolysis laser in this wavelength region, particularly from the measurement of partial cross sections and the dependence of β on the photolysis wavelength.

6. Conclusions

Using the method of polarised high resolution photofragment translational spectroscopy we have been able to determine the recoil anisotropy parameter β as a function of photofragment translational energy. The results show a decreasing trend of β with decreasing translational energy, which is particularly pronounced in the region where the signals from the dissociation channels producing $S(^1D)$ and $S(^3P)$ overlap. This behaviour is accounted for by partitioning the photofragment signal into two components with constant β corresponding to the formation of $S(^3P)$ and $S(^1D)$, respectively. Using the branching ratio $S(^3P)/S(^1D) \approx 3$ determined by Waller and Hepburn [18] as an additional piece of information, the component anisotropy parameters $\beta(S\ ^3P) \approx 1.0$ and $\beta(S\ ^1D) \approx 0.2$ were obtained from our experimental data with Ne carrier gas. In the case of He carrier gas $\beta(S\ ^3P)$ is somewhat lower than with neon. All these findings can be rationalised if one assumes that the overall photodissociation process occurs on a time scale of ~ 1.5 ps, which is approximately three times longer than the

the lifetime of the $\tilde{A}$ state photoexcited at 205 nm [16]. This indicates that the time required for the overall photodissociation process of CS_2 is substantially longer than the lifetime of the $\tilde{A}$ state. Finally, our results indicate that the formation of CS + $S(^1D)$ proceeds through a strongly bent transition state, in contrast to the formation of CS + $S(^3P)$.

Acknowledgement

Support by the Schweizerischer Nationalfonds zur Förderung der wissenschaftlichen Forschung and by the Alfred Werner Legat is gratefully acknowledged. The authors are indebted to Professor J.R. Huber for his generous support and for many stimulating discussions. JGF thanks the Ciba Fellowship Trust for an ACE award.

References

[1] R. Schinke, K. Weide, B. Heumann and V. Engel, Faraday Discussions Chem Soc. 91 (1991) 31, and references therein.
[2] R.L. Miller, S.H. Kable, P.L. Houston and I. Burak, J. Chem. Phys. 96 (1992) 332.
[3] A. Stolow and Y.T. Lee, J. Chem. Phys. 98 (1993) 2066.
[4] G.P. Morley, I.R. Lambert, M.N.R. Ashfold, K.N. Rossner and C. Western, J. Chem. Phys. 97 (1992) 3157.
[5] P. Felder, B.-M. Haas and J.R. Huber, Chem. Phys. Letters 204 (1993) 248.
[6] V. Engel, V. Staemmler, R.L. Vander Wal, F.F. Crim, R.J. Sension, B. Hudson, P. Andresen, S. Hennig, K. Weide and R. Schinke, J. Phys. Chem. 96 (1991) 3201.
[7] A. Ogai, J. Brandon, H. Reisler, H.U. Suter, J.R. Huber, M.v. Dirke and R. Schinke, J. Chem. Phys. 96 (1992) 6643.
[8] H.U. Suter, J.R. Huber, M.v. Dirke, A. Untch and R. Schinke, J. Chem. Phys. 96 (1992) 6727.
[9] H.F. Davis and Y.T. Lee, J. Phys. Chem. 96 (1992) 5681.
[10] H.F. Davis, B. Kim, H.S. Johnston and Y.T. Lee, J. Phys. Chem. 97 (1993) 2172.
[11] C. Starrs, M.N. Jego, A. Mank and J.W. Hepburn, J. Chem. Phys. 96 (1992) 6526.
[12] A.E. Douglas and I. Zanon, Can. J. Phys. 42 (1964) 627.
[13] J.W. Rabalais, J.M. McDonald, V. Scherr and S.P. McGlynn, Chem. Rev. 71 (1971) 73.
[14] K. Hara and D. Phillips, J. Chem. Soc. Faraday Trans. II 74 (1978) 1441.
[15] A.P. Baronawski and J.C. Owrutsky, Chem. Phys. Letters 221 (1994) 419.
[16] H.T. Liou, P. Dan, T.Y. Hsu, H. Yang and H.M. Lin, Chem. Phys. Letters 192 (1992) 560.
[17] S. Yang, A. Freedman, M. Kawasaki and R. Bersohn, J. Chem. Phys. 72 (1980) 4048.
[18] I.M. Waller and J.W. Hepburn, J. Chem. Phys. 87 (1987) 3261.
[19] B. Li and A.B. Myers, J. Chem. Phys. 94 (1991) 2458.
[20] V.R. McCrary, R. Lu, D. Zakheim, J.A. Russell, J.B. Halpern and W.M. Jackson, J. Chem. Phys. 83 (1985) 3481.
[21] M.D. Barry, N.P. Johnson and P.A. Gorry, J. Phys. E 19 (1986) 815.
[22] W.B. Tzeng, H.M. Yin, W.Y. Leung, J.Y. Luo, S. Nourbakhsh, G.D. Flesch and C.Y. Ng, J. Chem. Phys. 88 (1988) 1658.
[23] H. Kanamori and E. Hirota, J. Chem. Phys. 86 (1987) 3901.
[24] J.E. Butler, W.S. Drozdoski and J.R. McDonald, Chem. Phys. 50 (1980) 413.
[25] G.G. Balint-Kurti and M. Shapiro, Chem. Phys. 61 (1981) 137.
[26] S.J. Singer, K.F. Freed and Y. Band, J. Chem. Phys. 79 (1983) 6060.
[27] J.R. Waldeck, M. Shapiro and R. Bersohn, J. Chem. Phys. 99 (1993) 5924.
[28] P. Felder, Chem. Phys. 143 (1990) 141.
[29] P. Felder, Habilitationsschrift, Universität Zürich, Zürich, (1993).
[30] T.K. Minton, P. Felder, R.J. Brudzynski and Y.T. Lee, J. Chem. Phys. 81 (1984) 1759.
[31] R.N. Zare, Mol. Photochem. 4 (1972) 1.
[32] J.G. Frey, Mol. Phys. 79 (1993) 1287.
[33] R.K. Sparks, K. Shobatake, L.R. Carlson and Y.T. Lee, J. Chem. Phys. 75 (1981) 3838.
[34] G.E. Busch and K.R. Wilson, J. Chem. Phys. 56 (1972) 3638.
[35] I. Levy and M. Shapiro, J. Chem. Phys. 89 (1988) 2900.
[36] J.G. Frey and P. Felder, Mol. Phys. 75 (1992) 1419.
[37] H. Okabe, J. Chem. Phys. 56 (1972) 4381.
[38] JANAF Thermochemical Tables, J. Phys. Chem. Ref. Data Suppl. 1 14 (1985).
[39] P. Felder, Chem. Phys. 155 (1991) 435.
[40] B.-M. Haas, P. Felder and J.R. Huber, Chem. Phys. Letters 180 (1991) 293.
[41] D.T. Cramb, H. Bitto and J.R. Huber, J. Chem. Phys. 96 (1992) 8761.
[42] G.M. McClelland, K.L. Saenger, J.J. Valentini and D.R. Herschbach, J. Phys. Chem. 83 (1979) 947.
[43] C. Jonah, J. Chem. Phys. 55 (1971) 1915.
[44] S. Yang and R. Bersohn, J. Chem. Phys. 61 (1974) 4400.